Effects of epidemiological structure on the transient evolution of HIV virulence

Sang Woo Park and Ben Bolker

May 13, 2016

Abstract

The evolutionary dynamics of parasite virulence over the course of an emerging epidemic have important implications both for our basic understanding of epidemiological dynamics and, potentially, for the outcomes of public health interventions. In general changes in fitness landscapes over the course of an epidemic will select for higher virulence during the early, exponential-growth phase of the epidemic, but quantitative outcomes can depend sensitively on biological details and the structure of mathematical models used to capture them. Fraser, Shirreff, and co-workers have proposed a series of models for eco-evolutionary dynamics of HIV that are relatively detailed in their portrayal of the tradeoffs between transmission and virulence (mediated by set-point viral load, SPVL) and their heritability between hosts. However, these models use very simple implicit representations of the transmission process that ignore the partnership dynamics that previous research has found to be critical in predicting epidemics of sexually transmitted diseases. We explore models that combine HIV virulence tradeoffs with a range of epidemiological structures, modeling partnership formation and dissolution and allowing for individuals to transmit disease outside of partnerships. We assess summary statistics such as the peak value of virulence (SPVL) and the time at which the peak occurs across all models and across a Latin hypercube sample that captures a realistic range of partnership dynamic parameters for sub-Saharan Africa. In order to account for the different interpretations of parameters across model structures, we scale all parameter sets to constrain the simulated epidemic growth rate to be identical, matching a realistic baseline value. Our primary result is that, for this particular model setting, the simplest random-mixing structure is actually the best approximation to the most realistic model; this surprising outcome occurs because the dominance of extra-pair contact in the realistic model tends to mask the effects of partnership structure.

1 Introduction

The evolution of pathogen virulence is a fundamental process in evolutionary biology, of both theoretical and (potentially) practical importance.

The trade-off theory (Ebert, 1999) — which postulates that parasite virulence can be explained as the long-term evolutionary outcome of a saturating relationship between parasite clearance rate and transmission rate — has been criticized (Ebert and Bull, 2003; Alizon and Michalakis, 2015), but has also been successfully applied in a variety of host-pathogen systems (Dwyer et al., 1990; Mackinnon and Read, 1999; Jensen et al., 2006; De Roode et al., 2008). One particularly interesting application of these ideas is the work by Fraser et al. showing that HIV appears to satisfy the prerequisites of the tradeoff theory: in a study of discordant couples (i.e. long-term sexual partnerships with one infected and one uninfected partner), HIV virulence as measured by the rate of progression to AIDS was both heritable and covaried with the set-point viral load (i.e., the characteristic virus load measured in blood during the intermediate stage of infection), which in turn predicted the probability of within-couple transmission (Fraser et al., 2007, 2014). Subsequent studies (Shirreff et al., 2011; Herbeck et al., 2014) used these data to parameterize mechanistic models of HIV virulence evolution, suggesting that HIV invading a novel population would initially evolve increased virulence, peaking after approximately [XXX] years and then declining slightly to a long-stable virulence level.

read/check fraser+ 2014!; check vs. Herbeck et al. (2012)

The work of Shirreff et al., and particularly the predicted transient peak in HIV virulence midway through the epidemic, highlights the importance of interactions between epidemiological and evolutionary factors (Day and Proulx, 2004; Alizon, 2009). However, despite the attention to mechanistic detail at the individual or physiological level, the epidemiological structures used in these models are relatively simple.

Gras et al. (2009) and Müller et al. (2009) say that mean virulence has been increasing in Netherlands and Italy. Empirical support? Worth checking out maybe? I think these are similar to what Herbeck et al. (2012) says about the evolutionary trend but more specific...

As we discuss in detail below, the existing models of HIV eco-evolutionary dynamics either use implicit models that incorporate the average effects of within-couple sexual contact — without representing the explicit dynamics of pair formation and dissolution or accounting for extra-partnership contact — or use an agent-based formulation with parameters that effectively lead to random mixing among infected and uninfected individuals. Here we explore the effects of incorporating *explicit* epidemiological structure in eco-evolutionary models.

Lythgoe et al. (2013) — multi-strain model + within host dynamics but assumes random mixing. This one considers multi-strains existing within a host. Another complication that is important but this paper also ignores the partnership dynamics...

We add complexity to the epidemiological model following the general approach of Champredon et al. (2013); individuals join and leave partnerships at a specified rate, and can have sexual contact both within and outside of established partnerships. At the same time, our analysis somewhat simplifies the models of Shirreff et al., for computational tractability; we check that our qualitative results are not sensitive to these simplifications. In order to explore how virulence evolution depends on epidemiological structure, we consider a series of models with increasing levels of complexity. In order to avoid dependence of the results on a particular set of parameters — as we explain below, finding matching sets of parameters across models with widely differing epidemiological structures is challenging — we evaluate our models across a wide range of parameters, again following Champredon et al. in using a Latin hypercube design. For each

van Dorp et al. (2014) — seems even more complicated but doesn't seem like it mentions anything about partnership dynamics... HIV phases are based on Fraser and Hollingsworth et al

Herbeck et al. (2016) — seems better than the previous herbeck et al paper but still weird and is not published (bioRxiv)..

model run, we compute a set of metrics (peak virulence, timing of virulence peak, equilibrium virulence) that summarize the evolutionary trajectory of a simulated HIV epidemic.

2 Methods

more papers on SPVL heritability (*maybe* include): Alizon et al. (2010); Leventhal and Bonhoeffer (2016)

As our primary goal is to explore how different epidemiological structures (i.e. partnership dynamics and contact structures) affect our conclusions about the evolution of virulence, our models use a simplified description of within-host dynamics and heritability derived from Shirreff et al.'s multi-strain evolutionary model. Like Shirreff et al., we use a simple susceptible-infected-susceptible demographic formulation; rather than modeling birth and death (or more specifically, recruitment into the sexually active population and death), we assume that whenever an individual dies from infection, another enters the susceptible compartment.

2.0.1 Infection dynamics

Like Shirreff et al., we focus on the evolution of mean $\log_{10}$ set-point viral load, SPVL (which we denote as α), rather than virulence (i.e. rate of progression to AIDS) itself. In contrast to Shirreff et al., we use a single-stage disease model instead of accounting explicitly for progression through the three main stages of HIV infection (primary, asymptomatic, and disease), and we use a simple exponentially distributed infectious period instead of a more realistic Weibull-distributed infectious period. We account for varying transmission rates and durations of each disease stage by summing the durations of three stages (again based on Shirreff et al.'s model) and taking the duration-weighted average of transmission rates of three stages. Thus the within-couple transmission rate, β, for our models is given by:

$$\beta(\alpha) = \frac{D_P\beta_P + D_A(\alpha)\beta_A(\alpha) + D_D\beta_D}{D_P + D_A(\alpha) + D_D} \tag{1}$$

where the duration of infection (D_P and D_D) and rate of transmission (β_P and β_D) of the **P**rimary and **D**isease stages of infection are independent of the host's SPVL. Following Shirreff et al., the duration of infection (D_A) and rate of transmission (β_A) for the **A**symptomatic stage are Hill functions of the SPVL:

$$\begin{aligned} D_A(\alpha) &= \frac{D_{\max} D_{50}^{D_k}}{V_\alpha^{D_k} + D_{50}^{D_k}}, \\ \beta_A(\alpha) &= \frac{\beta_{\max} V_\alpha^{\beta_k}}{V_\alpha^{\beta_k} + \beta_{50}^{\beta_k}}, \end{aligned} \tag{2}$$

where $V_\alpha = 10^\alpha$. The **u**ncoupled and **e**xtra-couple transmission rates are scaled by multiplying the **w**ithin-couple transmission rate β by the contact ratios c_u/c_w and c_e/c_w.

2.0.2 Mutation

Like Shirreff et al. we incorporate a between-host mutation process in the SPVL, but simplify Shirreff et al.'s evolutionary model slightly by using a one-to-one genotype-phenotype mapping. The mutational process in our model is directly taken from Shirreff et al.. Over the course of infection, mutation occurs within the host. However, it is assumed that SPVL of an infected individual is determined by the SPVL at the time of infection for simplicity (and is not further affected by within-host mutation). Instead, the mutational effect takes place when an infected individual transmits the virus to a susceptible individual. First, the distribution of $\log_{10}$ SPVL is discretized into a vector:

$$\alpha_i = (\alpha_{\max} - \alpha_{\min})\frac{(i-1)}{n-1} + \alpha_{\min} \qquad i = 1, 2, 3, \ldots n. \tag{3}$$

We have experimented with varying degrees of discretization in the strain distribution (i.e., values of n); in our model runs comparing results with Shirreff et al. (2011) (Figure 1) we use $n = 51$ (i.e. a bin width of 0.05 $\log_{10}$ SPVL for α), but we find only small differences when reducing n to 21 (bin width 0.25 $\log_{10}$ SPVL), which we use for all other simulations.

We construct an n by n mutational matrix, M — which is multiplied with the transmission term — so that M_{ij} is the probability that a newly infected individual will have $\log_{10}$ SPVL of α_j given that the infector has $\log_{10}$ SPVL of α_i. Finally, the probabilities are normalized so that each row sums to 1:

$$M_{ij} = \frac{\Phi(\alpha_j + d/2; i) - \Phi(\alpha_j - d/2; i)}{\Phi(\alpha_{\max} + d/2; i) - \Phi(\alpha_{\min} - d/2; i)}, \tag{4}$$

where $\Phi(x; i)$ is the Gaussian cumulative distribution function with mean α_i and variance of σ_M^2, and $d = (\alpha_{\max} - \alpha_{\min})/(n-1)$. Transmission rate and disease induced mortality rates are discretized into a vector as well:

$$\begin{aligned} \beta_i &= \beta(\alpha_i) \\ \lambda_i &= \frac{1}{D_P + D_A(\alpha_i) + D_D} \end{aligned} \tag{5}$$

2.0.3 Contact structure and partnership dynamics

We developed six multi-strain evolutionary models, designed to cover a gamut between Champredon et al.'s relatively realistic and Shirreff et al.'s relatively simplistic epidemiological structures, each of which is based on different assumptions regarding contact structure and partnership dynamics. Specifically, we focus on the effects of the assumptions of (1) instantaneous vs. non-instantaneous partnership formation and (2) zero vs. positive extra-partnership sexual contact and transmission on the evolution of mean $\log_{10}$ SPVL.

Our first four models consider explicit partnership dynamics and are based on Champredon et al.'s model. Models 1 and 2 assume non-instantaneous partnership formation (i.e. individuals spend some time uncoupled, outside of partnerships) and consist of five states that are classified by infection status and partnership status. S is the number of single (uncoupled)

susceptible individuals, and I is the number of single infected individuals. SS is the number of susceptible-susceptible couples, SI is the number of serodiscordant (susceptible-infected) couples, and II is the number of concordant positive (infected-infected) couples. Model 1 includes extra-partnership contact (with both uncoupled individuals and individuals in other partnerships) whereas model 2 only considers within-couple transmission. Models 3 and 4 assume instantaneous partnership formation and thus consist of only the three partnered states: SS, SI, and II. Parallel to model 1 and 2, model 3 includes extra-partnership contact (now only with individuals in other partnerships, since uncoupled individuals don't exist in this model) and model 4 only considers within-couple transmission.

In contrast, models 5 and 6 are not explicitly structured. Model 5 is an implicit serial monogamy model based on the epidemiological model used by Shirreff et al.. It is actually a random mixing model that consist of only two states, S and I, and does not consider explicit partnership dynamics. However, to simulate the effect of instantaneous partnership formation, it uses an adjusted transmission rate that is derived from approximated basic reproduction number of a serial monogamy model (Hollingsworth et al., 2008). Finally, model 6 is a simple random-mixing model.

cite?

The base model (i.e. model 1) for the first four models is an extension of Champredon et al.'s model. Individuals in single compartment acquire a partner at a rate, ρ, and partnerships dissolve at a rate, c. Infected individuals in a discordant partnership infect susceptible partner at a rate β (within-couple transmission rate) and susceptible individuals outside the partnership at a rate c_e (extra-couple transmission rate). Likewise, a single infected individual can infect any susceptible individuals at a rate c_u through uncoupled mixing. Extra-couple and uncoupled transmission are modeled in a same way as Champredon et al.'s model. All the details have been adapted to a multi-strain scenario. Model 2, 3, and 4 are derived from the base model by removing epidemiological details (partnership formation and uncoupled/extra-couple contact). Model details are explained in the appendix.

2.1 Latin hypercube sampling

Despite considerable effort by many researchers (e.g. Hollingsworth et al., 2008; Champredon et al., 2013), the parameters determining the rate and structure of sexual partnership change and contact are still very uncertain; this led Champredon et al. to adopt a Latin hypercube sampling (LHS) strategy (Blower et al., 1991) that evaluates model outcomes over a range of parameter values. In order to make sure that our comparisons among models apply across the entire space of reasonable parameter values, and in order to evaluate the differential sensitivity of different model structures to parameter values, we follow a similar protocol and perform LHS over a parameter set including both the transmission and duration parameters (β_P, D_P, β_D, D_D) and contact/partnership parameters (ρ, c, c_u/c_w, and c_e/c_w). We do not allow for uncertainties in parameters that are directly related to the evolutionary process ($\beta_{\max}$, β_{50}, β_k, $D_{\max}$, D_{50}, D_k, σ_M), using Shirreff et al.'s point estimates throughout.

Latin hypercube sampling is done as in Champredon et al.. For each

parameter, z, its range is divided into $N = 1000$ equal intervals on a log scale:

$$z_i = \exp\left(\log(z_{\min}) + [\log(z_{\max}) - \log(z_{\min})]\frac{i-1}{N-1}\right) \qquad i = 1, ..., N. \quad (6)$$

For simplicity, we assume that all parameters are uniformly distributed on the log scale. Following the vectorization of a parameter range, a matrix is constructed so that each column contains a vector of a parameter series which it represents (z_1,...z_N). Then, each column is replaced with a random permutation series of itself. Now, each row contains a different parameter set that is used for each simulation run.

Table 1 gives the ranges of the model parameters used for LHS. Parameter ranges regarding contact and partnership dynamics (ρ, c, and c_e/c_w) are taken from Champredon et al., whereas those regarding infection (β_P, D_P, β_D, and D_D) are taken from Hollingsworth et al. (2008). The remaining parameters are taken from Shirreff et al..

The one completely new parameter in our model, the ratio of uncoupled to within-couple transmission c_u/c_w, is needed to more flexibly contrast uncoupled and extra-couple transmission dynamics within multi-strain models (Appendix); we need to pick a reasonable range for it. Champredon et al. assume that the effective within-couple contact rate and effective uncoupled contact rate have the same range of 0.05 - 0.25. Given Champredon et al.'s parameter range, the possible maximum and minimum values of c_u/c_w are 5 and $1/5$. Therefore, we use $1/5$-5 as the range for the parameter c_u/c_w. Although this adds more uncertainty to the parameter c_u — Champredon et al.'s range implies a 5-fold difference whereas ours gives a 25-fold difference — as there is not much known about the uncoupled transmission rate, we consider the wider range appropriate.

2.2 Simulation runs

One of the most difficult parts of model comparison is finding parameter sets that are commensurate against many different model structures. For the most part, our models are too complex to easily derive analytical correspondences among them. Given a numerical criterion, such as r (initial exponential growth rate) or $\mathcal{R}_0$ (intrinsic reproductive number), we can adjust one or more parameters by brute force to ensure that all of the models match according to that criterion. While $\mathcal{R}_0$ is often considered the most fundamental property of an epidemic, and might thus seem to be a natural goal, here we focus on matching the initial growth rate r for several reasons. First, our primary interest is in the transient evolutionary dynamics of virulence, which are more strongly affected by r than $\mathcal{R}_0$. Second, r is in general more directly observable in real epidemics; r can be estimated by simply fitting an exponential curve to the initial incidence or prevalence curves (Ma et al., 2014), while $\mathcal{R}_0$ typically requires either (1) knowledge of *all* epidemic parameters or (2) relatively sophisticated back-calculation based on r and knowledge of the serial interval or generation interval of the disease (Wallinga and Lipsitch, 2007). Thus, we scale a parameter so that every run has the same initial exponential growth rate in the incidence.

In order to allow for all models to have equal initial exponential growth rate, r, we need to pick a parameter, s, so that $\lim_{s\to 0} r(s) = 0$ and $\lim_{s\to\infty} r(s) = \infty$. As adjusting either partnership change rate (i.e. partnership formation and dissolution rate) or transmission rate does not fulfill this requirement for certain models, we decided to scale partnership change rate and dissolution rate by the same factor of γ: $\beta_{\text{adj}} = \gamma\beta_{\text{base}}$, $c_{\text{adj}} = \gamma c_{\text{base}}$, $\rho_{\text{adj}} = \gamma\rho_{\text{base}}$. Since transmission rate is adjusted by the scale of γ, uncoupled and extra-couple transmission rates are adjusted as well. For models 3, 4, and 5, all of which assume instantaneous partnership (and hence do not track single individuals), only the transmission rate and partnership dissolution rate (in this case equivalent to the partnership change rate) are adjusted.

We run each model for each of 1000 parameter sets chosen by Latin hypercube sampling , with fixed starting conditions of mean $\log_{10}$ SPVL of 3 and epidemic size of 10^{-4}. After each run, initial exponential growth rate is calculated. Then, parameters are scaled so that the initial exponential growth rate is scaled to 0.04, which is approximately equal to that of Shirreff et al's model.

CITE Blower et al - or at first mention of LHS

For each model we derive the following summary statistics: peak virulence, peak time, equilibrium virulence, and relative peak virulence. The transient phase of an epidemic is often characterized by high virulence, and we define peak virulence as the maximum virulence during this phase. It is simply calculated by taking the maximum value from the virulence trajectory, and peak time is the time at which the maximum value is reached. Once the epidemic enters the endemic phase, evolution of virulence stabilizes and reaches equilibrium. Equilibrium virulence is calculated by taking the mean virulence at 4000 years. Although most simulations reach equilibrium much earlier, we set our time horizon at a much later date as some simulation runs have slow rate of evolution depending on the parameter set and model assumptions.

We focus on these statistics for the following two reasons. First of all, knowing the possible ranges for the peak virulence allows us to estimate the worst-case scenario for the HIV and other sexually transmitted disease epidemics. Pathogens may already have evolved towards high virulence during the early stages of an epidemic, by the time it is observed by public health authorities. Understanding how virulent a pathogen can evolve before an epidemic begins can be helpful for controlling the disease. Furthermore, knowing the initial virulence, peak virulence, timing of the peak virulence, and equilibrium virulence provide sufficient detail to identify the shape of the virulence trajectory. During an epidemic outbreak, it is difficult to observe virulence evolution. Specifically, in the case of HIV and other sexually transmitted diseases, slow evolutionary time-scale makes observing changes in the mean virulence even more challenging. Knowing the ranges of these statistics can help real-time virulence evolution prediction during an epidemic less troublesome.

needs a bit of work

3 Results

Our simplifications of Shirreff et al.'s model reproduce its qualitative behaviour — in particular, its predictions of virulence dynamics — reason-

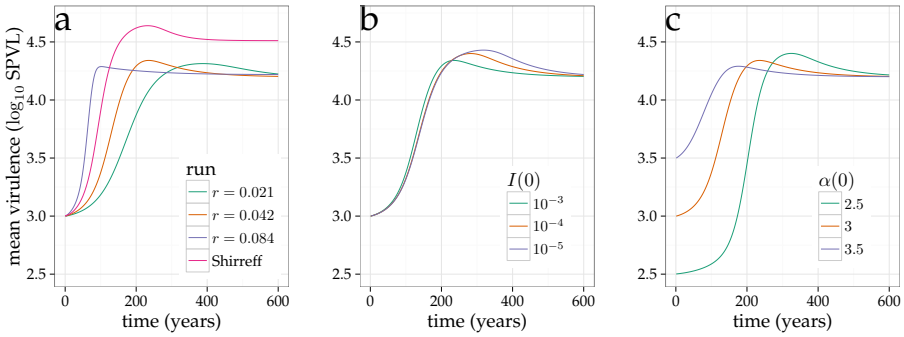

Figure 1: Baseline dynamics. Time series of mean population virulence ($\log_{10}$ SPVL). (a) Shirreff model, effects of varying r. (b) Effects of varying initial infectious density $I(0)$. (c) Effects of varying initial mean virulence $\alpha(0)$. Parameters

ably well. As r decreases from 0.084 to 0.42 (the latter value matching the initial rate of increase in prevalence in Shirreff et al.'s full model) the initial trajectory of increasing virulence brackets the rate from the original model (Figure 1a). However, our model produces lower peak virulence (≈ 4.3 vs. ≈ 4.6 $\log_{10}$ SPVL) and equilibrium virulence ≈ 4.25 vs. ≈ 4.5 $\log_{10}$ SPVL) than Shirreff's, even for matching initial incidence trajectories (i.e., $r = 0.042$ year^{-1}).

Changing the initial infectious density ($I(0)$), while it produces the expected changes in the initial epidemic trajectory (Supplementary material), has little effect on the virulence trajectory, making the virulence peaks slightly later and larger as $I(0)$ decreases. Decreasing $I(0)$ allows a longer epidemic phase before the transition to endemic dynamics (Figure 1b). Decreasing the initial virulence similarly but more strongly leads to progressively later, larger peaks in virulence (Figure 1c).

Across the entire range of parameters covered by the LHS analysis, all of the classes of models we considered produce qualitatively similar virulence trajectories (Figure 2). Although the speed of virulence evolution varies, leading to wide variation in the peak virulence (means ranging from approximately 3.75 to 4.5 $\log_{10}$ SPVL), virulence peaks in all models between 200 and 300 years.

Our chosen summary statistics (peak time, peak virulence, equilibrium virulence, and relative peak virulence) all vary considerably across models 3. We first consider the models of intermediate realism (implicit, instantaneous-switching with and without extra-pair contact, and pair formation without extra-pair contact). Some parameter sets for these models lead to low equilibrium virulence ($\approx 2.5 \log_{10}$ SPVL); these same sets lead to correspondingly low peak virulence ($< 3.5 \log_{10}$ SPVL) and early peak times (before 200 years), but high relative peaks (> 1.3) (Figure 4, leftmost column) because the equilibrium virulence is low. At the opposite extreme, parameter sets that produce high equilibrium virulence also produce late peaks ($>$ 200 years), high peak virulence, and low relative peaks (≈ 1.05). The

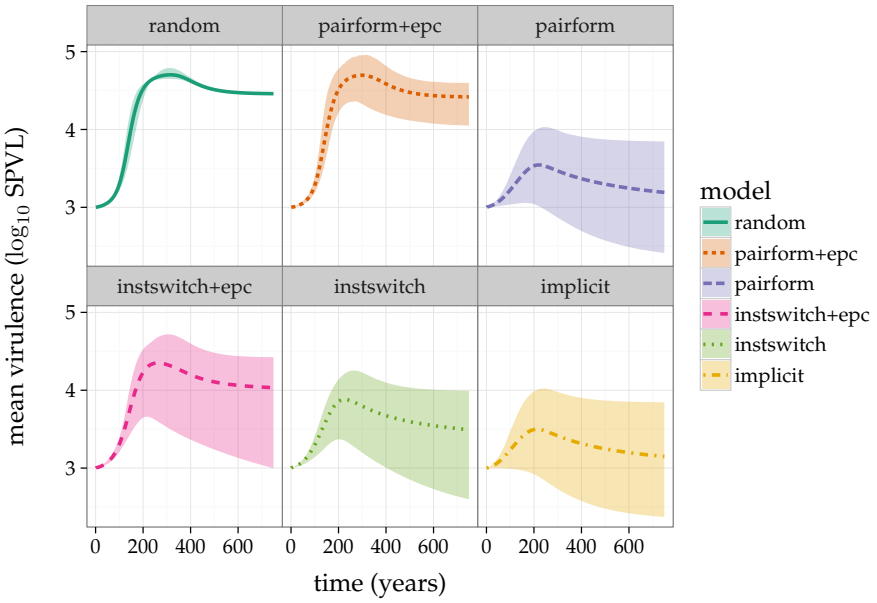

Figure 2: Envelopes of virulence trajectories under all models. All models were run until $t = 4000$ years; truncated series are shown here.

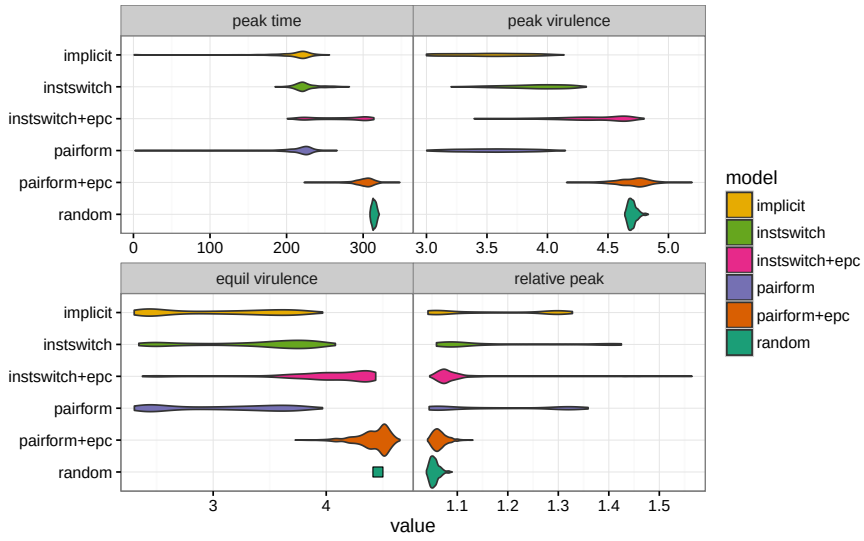

Figure 3: Univariate distributions of summary statistics. The distribution of equilibrium virulence for the random mixing model is very narrow, and has been replaced by a point in order to preserve the vertical axis scaling.

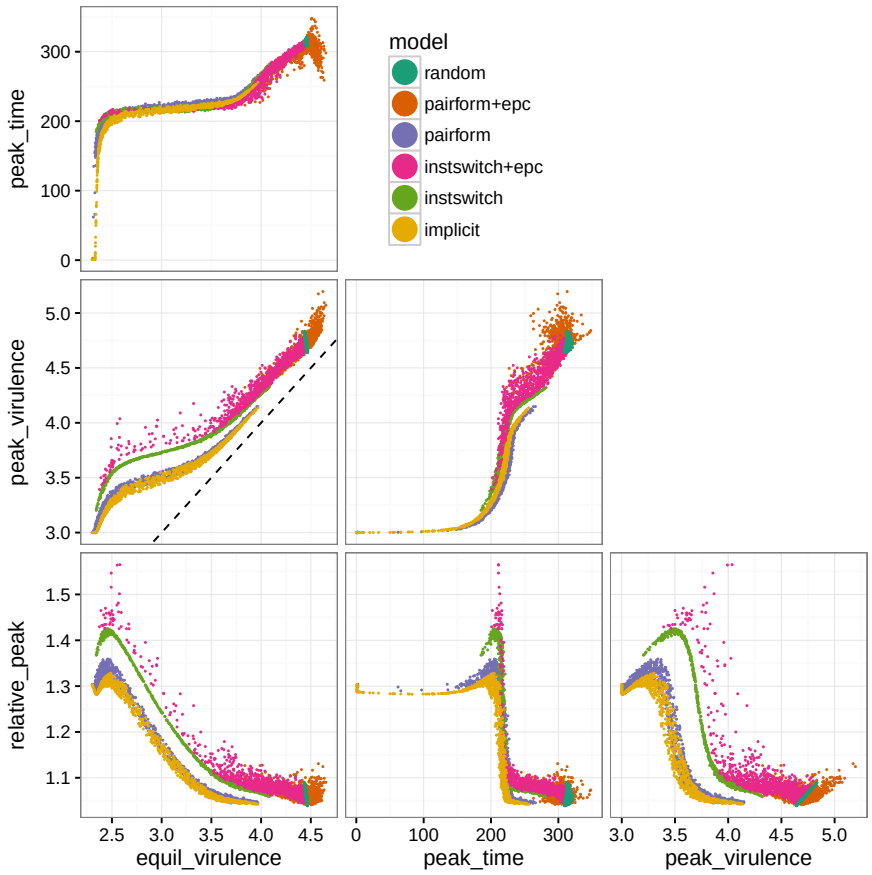

Figure 4: Pairs plot: bivariate relationships among summary statistics for each model structure. Dashed line in equilibrium vs. peak virulence plot shows 1:1 line.

pair-formation without extra-pair contact and implicit models occasionally have parameter sets that select for such low virulence across the board that they never exceed their initial virulence, leading to a tail of peak times near zero.

The most striking aspect of the univariate comparisons in Figure 3, (and the bivariate comparisons in Figure 4) is the match between the output of the least (random mixing) and the most complex (pair formation with extra-pair contact) models. The random-mixing model has lower variability, because it is unaffected by uncertainty in pair formation and extra-pair contact parameters, but otherwise the virulence dynamics of these two extreme models are remarkably similar. This phenomenon is driven by the strength of extra-pair contact in the model with explicit pair formation and extra-pair contact ("pairform+epc" in Figures 2-5). When individuals spend time uncoupled between partnerships, and when these single individuals can transmit disease to coupled individuals, the resulting unstructured mixing overwhelms the effect of structured mixing within couples, leading to mixing that is effectively close to random.

Plotting the bivariate result distributions (Figure 4) shows that most of the relationships among the summary statistics are monotonic, except those involving the relative peak virulence (bottom row). Changes in parameters that increase the equilibrium virulence initially increase the peak virulence even more, so that the relative peak virulence increases as well, but beyond an equilibrium virulence of about 2.5 $\log_{10}$ SPVL the peak virulence increases slower than the equilibrium virulence, leading to a decrease in the relative peak virulence.

The bivariate relationships also help distinguish the results of different models with similar univariate distributions. While the relationship between equilibrium virulence and peak time is similar for all model structures (top left panel), the other relationships are more separate. In particular, the implicit and pair-formation (without extra-pair contact) are very similar to each other, but distinct from the other models. We still do not have a convincing explanation for this distinction; we would have expected the implicit model to be most similar to the the instantaneous-switching model without extra-pair contact, which most closely matches its derivation. However, we note that the implicit model derivation is based on defining the force of infection to match a scaled version of $\mathcal{R}_0$, and as such would be expected to match the equilibrium behaviour but not necessarily the epidemic-phase behaviour of a model with explicit partnership dynamics.

Finally, the sensitivity plots (Figure 5) show the effects of each parameter on the summary statistics. In almost every case the effects of the parameters are monotonic; note that the plot shows the effects of the *unscaled* parameters, i.e. before they have been adjusted to achieve a standard initial epidemic growth rate. Increases in the transmission rates (β_P, β_D) and durations (D_P, D_D) in the primary and disease stages generally decrease the equilibrium virulence, peak virulence, and peak time, although the random and pair-formation+extra-pair contact models have high, relatively constant values with respect to these parameters.

The base contact rate increases virulence and peak time in almost all cases, although the pair-formation+extra-pair contact model is again rel-

better explanation of why increasing β/D and then scaling r should lead to lower $\mathcal{R}_0$?

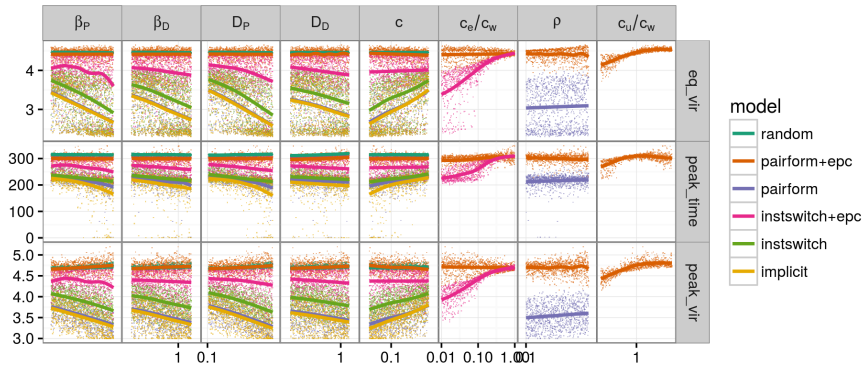

Figure 5: Sensitivity plot. For each parameter in the Latin hypercube sample and each summary statistic, shows the distribution (points) and trend (smooth line) of the summary statistic as a function of the *unscaled* parameter value, i.e. prior to adjusting the parameters to achieve the standard initial epidemic growth rate.

atively insensitive. The ratio of extra-pair to within-pair contact (c_e/c_w) affects virulence in the instantaneous-switching+epc model, but not the pair-formation+epc model (probably because the uncoupled individuals present in the pair-formation+epc model make extra-pair contact by coupled individuals less important). Surprisingly, neither of the pair-formation models is particularly sensitive to the rate of partnership formation (ρ); the rate of uncoupled contact increases virulence and peak time in the pair-formation+epc model, which is the only model to which it applies.

4 Discussion

All models must simplify the world. Many constraints — such as data availability, computation time, or code complexity — drive the need for parsimony, with different constraints applying in different contexts. The critical question that modelers must ask is whether the simplified model gives adequate answers, or whether the simplifications have led to qualitatively or quantitatively incorrect conclusions. This question is especially important for modelers who are hoping that their conclusions will guide management decisions.

In the particular example of HIV virulence eco-evolutionary dynamics and epidemiological, we reach the slightly ironic conclusion that the effort put into building a more realistic model essentially cancels out, leaving us in the same position as if we had ignored the problem of epidemiological complexity entirely and used a naive random-mixing contact model. Herbeck et al. (2014) build a network model of partnerships, but they set the "partnership" duration to 1 day — very unrealistic in epidemic terms, but perhaps actually more true to real-world HIV epidemiological dynamics

than a model with realistic partnership durations that neglects extra-pair contact (Herbeck et al., 2016). Adding still further realism might push the results farther away from the random-mixing model. For example, our model forms partnerships randomly, and assumes that extra-pair contact is randomly mixing across the population; one could instead implement extra-pair contact as arising from multiple concurrent partnerships (some, such as contact with sex workers, of very short duration), or more structured partnership formation (by age, ethnicity, or behaviour group). The effects of other realistic complications such as explicit modeling of two sexes (both in contact structure and differential transmission probabilities), temporal and spatial variation in epidemic processes, or presence of genetic variation in hosts are harder to predict.

Parameterization is one of the biggest challenges of epidemiological modeling. In addition to following Champredon et al. (2013) by doing Latin hypercube sampling across a wide range of epidemiological parameters, we calibrated each set of parameters to the same initial epidemic growth rate, chosen to match the results of previous models (Shirreff et al., 2011). The previous models drew their parameters from previous cohort studies from the 1990s (Wawer et al., 2005; Hollingsworth et al., 2008) rather than doing any explicit calibration to epidemic curves, but they give reasonable order-of-magnitude growth rates (≈ 0.04 year^{-1}) for the early stages of the HIV epidemic (although considerably lower than estimates of $\approx 0.07 - 0.1$ year^{-1} based on population genetic reconstructions (Faria et al., 2014)). However, our reason for calibrating was not to match any specific observed epidemic, but rather to make sure that we were making meaningful comparisons across a range of models with radically different epidemiological structures, and hence involving different interpretations of the same quantitative parameters. For example, in models with instantaneous switching the partnership dissolution rate c is identical to the partnership formation rate; in models with explicit partnership formation, the partnership formation rate is also c at equilibrium, but might vary over the course of an epidemic. It is not obvious whether models with equal parameters but different structures should be directly compared; calibration solves this problem.

do we know what r Champredon et al. get?? They give a really wide range of values so I'm not sure...

Not really sure what this example means...

More generally, any model that wants to be taken seriously for management and forecasting purposes should be calibrated to *all* available data, using informative priors to incorporate both realistic distributions of uncertainty for all parameters from independent measurements (Elderd et al., 2006) and calibration from population-level observations of epidemic trajectories. For practical (rather than exploratory) purposes, such a procedure would also be an improvement on the common — although not universal — practice of assessing uncertainty over uniform ranges, rather than distributions that allow more continuous variation in support over the range of a parameter.

Researchers have documented that HIV virulence and set-point viral load are changing, on time scales comparable to those portrayed here (e.g., compare Figure 2 to Herbeck et al. (2012)'s estimated rate of change of 1.3 $\log_{10}$ SPVL per century [95% CI -0.1 to 3]), and have begun to build relatively realistic models that attempt to describe how interventions such as mass antiretroviral therapy (ART) can be expected to change the tra-

jectory of virulence evolution (Payne et al., 2014; Herbeck et al., 2016). While these efforts are well-intentioned, we caution that epidemiological and other structural details that are currently omitted from these models could significantly change their conclusions.

5 To do

- use PLoS template for ms
- check on code/documentation on repo
- hard parts of the results:
  - explaining similarities among the models: why does implicit look most like pair formation model? (see R0comparison HTML)
  - explaining sensitivity plot
- cite Lipsitch and Nowak (1995)
- figures:
  - fig 1. tweak label position in (a)
  - fig 3. add units to strip labels?
  - fig 4. fix axis labels; squash panels together
  - fig 5. fix strip labels for summary statistics; fix x-axis labels
  - create fig A1 (scaled sensitivity plot) for supp materials

See Bolker JRSI Google scholar cites (alternative link)

A Model details

Since we use multi-strain models, in which the distribution of $\log_{10}$ SPVL has been discretized into a vector, we use a matrix notation to describe our models. The five states described in the Methods section are replaced with the following notations: S, I_i, SS, SI_i, II_{ij}, where the subscripts denote the strain that an individual is infected with. For example, I_i is number of infected individuals with $\log_{10}$ SPVL of α_i, and II_{ij} is the number of concordant, HIV-positive couples in which the two partners have $\log_{10}$ SPVL of α_i and α_j (independent of order; II_{ij} is synonymous with II_{ji}). Below, we use the Kronecker delta (i.e. $\delta_{ij} = 1$ if $i = j$ and 1 otherwise) in a slightly non-standard fashion as an exponent, e.g. $2^{\delta_{ij}}$, to set a value to 2 when $i = j$ and 1 otherwise.

Models 1 and 2: partnership dynamics

Single individuals acquire partners at rate ρ: $S' = -\rho S$ and $I_i' = -\rho I_i$. We follow Champredon et al's results and assume that single individuals are distributed into coupled states through binomial distribution:

? don't understand this wording (ditto below)

I think we need different notation for partnership formation (i.e. LHS is wrong)

$$
\begin{aligned}
(SS)' &= \frac{\rho S \cdot S}{2(S + \sum_k I_k)} \\
(SI_i)' &= \frac{\rho S \cdot I_i}{S + \sum_k I_k} \\
(II_{ij})' &= \left(\frac{1}{2}\right)^{\delta_{ij}} \cdot \frac{\rho I_i \cdot I_j}{S + \sum_k I_k}
\end{aligned}
\tag{7}
$$

In a single-strain model, both individuals in a concordant partnership, II, enter the single-infected compartment, I, when a partnership dissolves: $I' = 2cII'$. However, this is not the case in a multi-strain model. If infected individuals in an II partnership have different strains, they will enter different compartments; if they are both infected with the same strain, they both enter the same compartment. As described above, we use the Kronecker delta notation to implement this difference between the $i = j$ and $i \neq j$ cases.

Partnerships dissolve at rate c: $SS' = -cSS$, $SI_i' = -cSI_i$, and $II_{ij} = -cII_{ij}$. Unlike single strain model, where both individuals leaving the II partnership would enter I, we have to account for strains which the individuals in concordant partnership are infected with (i.e. both partners in II_{ii} enter I_i whereas only one partner in II_{ij} enters I_i).

$$
\begin{aligned}
S' &= 2cSS + \sum_k cSI_k \\
I_i' &= cSI_i + \sum_k 2^{\delta_{ik}} cII_{ik}
\end{aligned}
\tag{8}
$$

Combining partnership formation and dissolution process yields the following equation:

$$
\begin{aligned}
S' &= -\rho S + 2cSS + \sum_k cSI_k \\
I_i' &= -\rho I_i + cSI_i + \sum_k 2^{\delta_{ik}} cII_{ik} \\
SS' &= \frac{\rho S \cdot S}{2(S + \sum_k I_k)} - cSS \\
SI_i' &= \frac{\rho S \cdot I_i}{S + \sum_k I_k} - cSI_i \\
II_{ij}' &= \left(\frac{1}{2}\right)^{\delta_{ij}} \cdot \frac{\rho I_i \cdot I_j}{S + \sum_k I_k} - cII_{ij}
\end{aligned}
\tag{9}
$$

Models 1 and 2: infection

Within-couple transmission occurs in both models. An infected partner in SI partnership transmits virus to a susceptible partner, and partnership state becomes II: $SI_i' = -\beta_i SI_i$. Since we assume that mutation occurs, II_{ij}, where $i \neq j$, can be formed from both SI_i and SI_j partnership: $II_{ij}' = M_{ij}\beta_i SI_i + M_{ji}\beta_j SI_j$. On the other hand, II_{ii} can only be formed from an SI_i partnership: $II_{ii}' = M_{ii}\beta_i SI_i$. Using the Kronecker delta notation, we

obtain following set of equations that describe within-couple transmission dynamics:

$$\begin{aligned} SI_i' &= -\beta_i SI_i \\ II_{ij} &= \left(\frac{1}{2}\right)^{\delta_{ij}} \cdot (M_{ij}\beta_i SI_i + M_{ji}\beta_j SI_j) \end{aligned} \tag{10}$$

Champredon et al define the proportion of infectious extra-couple and uncoupled contact through the following term:

$$P = \frac{c_u I + c_e(SI + 2II)}{c_u(S + I) + 2c_e(SS + SI + II)}. \tag{11}$$

Effective uncoupled, c_u, and extra couple, c_e, contact rate is the product of two terms: uncoupled/extra-couple contact rate $\times$ rate of transmission per contact. Therefore, the transmission rate per contact term in c_u and c_e is canceled out in the equation above. Using this property, we modify the equation above as follows:

$$P = \frac{r_u I + r_e(SI + 2II)}{r_u(S + I) + 2r_e(SS + SI + II)}, \tag{12}$$

where $r_u = c_u/c_w$ and $r_e = c_e/c_w$ are the relative uncoupled/extra-couple contact rates. This simplification is useful in a multi-strain model since we cannot multiply a vector with a single value (e.g. $c_u S$ in denominator) if we use Champredon et al's equation in its original form. Extending the above equation to multi-strain model so that P_i represents the proportion of the extra-couple and uncoupled contact of an infected individual with strain i, we obtain:

$$P_i = \frac{r_u I_i + r_e(SI_i + \sum_k (II_{ik} + \delta_{ik} II_{ik}))}{r_u(S + \sum_k I_k) + r_e(2SS + \sum_k 2SI_k + \sum_l \sum_k (1 + \delta_{lk}) II_{lk})}, \tag{13}$$

Using the equation above, we can model uncoupled and extra-couple mixing. For convenience, uncoupled and extra-couple transmission rates, c_u and c_e, will be replaced with $U_i = r_u\beta_i$ and $E_i = r_e\beta_i$ hereafter.

Single susceptible individuals become infected and enter single infected compartment at the total rate of $\sum_k P_k U_k S$. Through mutation, newly infected individuals are distributed into single infected compartments with different strains: $I_i' = \sum_k M_{ki} P_k U_k S$. Either partner in an SS partnership can be infected, with the partnership state becoming SI, at the total rate of $\sum_i 2P_i E_i SS$. The formation of SI_i partnerships is similar to the process through which single susceptible individuals are distributed into single infected compartments: $SI_i' = \sum_k 2M_{ki} P_k E_k SS$. Lastly, the susceptible partner in an SI partnership can be infected due to uncoupled/extra-couple contacts and partnership can change to an II partnership. As in the previous cases, SI_i partnerships are lost at a rate of $\sum_k P_k E_k SI_i$. The mutation process is similar to that of within-couple transmission. The only difference is that the $\log_1 0$ SPVL of a newly infected partner is not determined by its social partner but from an extra-couple partner (i.e. the term P_i): $II_{ij}' = (1 - \frac{\delta_{ij}}{2})(\sum_k (M_{kj} P_k E_k SI_i + M_{ki} P_k E_k SI_j))$. Combining these equations we get the following set of equations that describe all the transmission dynamics

something missing here?

Model 1 and 2 - Disease induced mortality

The disease induced death rate, λ, is given by taking the reciprocal of the total duration of the infection: $\lambda_i = 1/(D_A + D_P(\alpha_i) + D_D)$. Since we assume an SIS formulation, where infected individuals that die from infection are immediately replaced by an individual in the single susceptible compartment, we obtain the following equation for single infected individuals:

$$\begin{aligned} S' &= \sum_k \lambda_k I_k \\ I_i &= -\lambda_i I_i \end{aligned} \tag{14}$$

If an infected individual in a partnership dies, the partnership dissolves. Thus, an SI_i partnership dissolves at a rate $-\lambda_i$, and the susceptible partner enters the single susceptible compartment at rate $\lambda_i SI_i$ (due to the SIS formulation the the infected partner that dies also gives rise, at an equal rate, to an individual entering the single susceptible compartment):

$$\begin{aligned} S' &= \sum_k 2\lambda_k SI_k \\ SI_i &= -\lambda_i SI_i \end{aligned} \tag{15}$$

Similarly, II_{ij} partnerships dissolve at a rate $-(\lambda_i + \lambda_j)$, but two cases, when $i \neq j$ and $i = j$, must be considered separately. When an II_{ij} partnership dissolves due to disease-induced mortality, where $i \neq j$, the death of the partner with strain i causes its partner to enter I_j compartment at rate $\lambda_j II_{ij}$, and vice versa. When an $II_i i$ partnership dissolves, the death of either partner causes the other partner to enter the I_i compartment at rate $\lambda_i II_{ii}$, which sums up to $2\lambda_i II_{ii}$. Combining these dynamics yields:

$$\begin{aligned} S' &= \sum_l \sum_k 2^{\delta_{lk}} \lambda_k II_{lk} \\ I_i' &= \sum_k 2^{\delta_{ik}} \lambda_k II_{ik} \\ II_{ij}' &= -(\lambda_i + \lambda_j) II_{ij} \end{aligned} \tag{16}$$

Finally, combining all these equations give us the full model, which is Model 1. We can simply take out the uncoupled and extra couple transmission term to obtain equation 2:

?

$$
\begin{aligned}
S' =& -\rho S + 2cSS + \sum_k cSI_k - \sum_k P_k U_k S + \sum_k \lambda_k I_k \\
&+ \sum_k 2\lambda_k SI_k + \sum_l \sum_k 2^{\delta_{lk}} \lambda_k II_{lk} \\
I_i' =& -\rho I_i + cSI_i + \sum_k 2^{\delta_{ik}} cII_{ik} + \sum_k M_{ki} P_k U_k S - \lambda_i I_i \\
&+ \sum_k 2^{\delta_{ik}} \lambda_k II_{ik} \\
SS' =& \frac{\rho S \cdot S}{2(S + \sum_k I_k)} - cSS - \sum_i 2P_i E_i SS \\
SI_i' =& \frac{\rho S \cdot I_i}{S + \sum_k I_k} - cSI_i - \beta_i SI_i + \sum_k 2M_{ki} P_k E_k SS - \sum_k P_k E_k SI_i \\
&- \lambda_i SI_i \\
II_{ij}' =& \left(\frac{1}{2}\right)^{\delta_{ij}} \cdot \frac{\rho I_i \cdot I_j}{(S + \sum_k I_k)} - cII_{ij} + \left(\frac{1}{2}\right)^{\delta_{ij}} \cdot (M_{ij}\beta_i SI_i + M_{ji}\beta_j SI_j) \\
&+ \left(\frac{1}{2}\right)^{\delta_{ij}} \cdot (\sum_k (M_{kj} P_k E_k SI_i + M_{ki} P_k E_k SI_j)) - (\lambda_i + \lambda_j) II_{ij}
\end{aligned}
\tag{17}
$$

Models 3 and 4: Partnership dynamics

Since model 3 and 4 assume instantaneous partnership formation, there are only three states: SS, SI_i, and II_{ij}. Partnership dissolution rates are equal to those of model 1 and 2: $SS' = -cSS$, $SI_i' = -cSI_i$, and $II_{ij}' = -II_{ij}$. Once individuals leave a partnership, they enter temporary compartments and are distributed into a partnership through binomial distribution:

$$
\begin{aligned}
X &= 2cSS + \sum_k cSI_k \\
Y_i &= cSI_i + \sum_k 2^{\delta_{ik}} cII_{ik} \\
SS' &= -cSS + \frac{X^2}{2(X + \sum_k Y_k)} \\
SI_i' &= -cSI_i + \frac{XY_i}{X + \sum_k Y_k} \\
II_{ij}' &= -cII_{ij} + \left(\frac{1}{2}\right)^{\delta_{ij}} \frac{Y_i Y_j}{X + \sum_k Y_k}.
\end{aligned}
\tag{18}
$$

Model 3 and 4 - Infection

Model 3 and 4 share the within-couple transmission term with model 1 and 2. Since there is no single state, only extra couple transmission exists:

$$
P_i = \frac{r_e(SI_i + \sum_k (II_{ik} + \delta_{ik} II_{ik}))}{r_e(2SS + \sum_k 2SI_k + \sum_l \sum_k (II_{lk} + \delta_{kl} II_{lk}))}. \tag{19}
$$

Movement from SS state to SI state and SI to SS is modeled through the same equation that is used in model 1 and 2.

Model 3 and 4 - Disease induced mortality

Disease induced mortality is modeled similar to model 1 and 2. However, as single state does not exist in model 3 and 4, individuals that has left their partnerships due to death of their partners enter temporary compartments and form partners instantly:

$$\begin{aligned} X &= \sum_k 2\lambda_k SI_k + \sum_l \sum_k 2^{\delta_{lk}} \lambda_k II_{lk} \\ Y_i &= \sum_k 2^{\delta_{ik}} \lambda_k II_{ik} \\ SS &= = \frac{X^2}{2(X + \sum_k Y_k)} \\ SI_i &= -\lambda_i SI_i + \frac{XY_i}{X + \sum_k Y_k} \\ II'_{ij} &= -(\lambda_i + \lambda_j) II_{ij} + \left(\frac{1}{2}\right)^{\delta_{ij}} \cdot \frac{Y_i Y_j}{X + \sum_k Y_k} \end{aligned} \tag{20}$$

Combining all these dynamics, we have equation 3. If we remove extra-couple transmission, we have equation 4.

$$\begin{aligned} X =& 2cSS + \sum_k cSI_k + \sum_k 2\lambda_k SI_k + \sum_l \sum_k 2^{\delta_{lk}} \lambda_k II_{lk} \\ Y_i =& cSI_i + \sum_k 2^{\delta_{ik}} cII_{ik} + \sum_k 2^{\delta_{ik}} \lambda_k II_{ik} \\ SS =& - cSS + \frac{X^2}{2(X + \sum_k Y_k)} - \sum_i 2P_i E_i SS \\ SI_i =& - cSI_i + \frac{XY_i}{X + \sum_k Y_k} - \beta_i SI_i + \sum_k 2M_{ki} P_k E_k SS \\ & - \sum_k P_k E_k SI_i - \lambda_i SI_i \\ II_{ij} & - cII_{ij} + \left(\frac{1}{2}\right)^{\delta_{ij}} \frac{Y_i Y_j}{X + \sum_k Y_k} + \left(\frac{1}{2}\right)^{\delta_{ij}} \cdot (M_{ij}\beta_i SI_i + M_{ji}\beta_j SI_j) \\ & + \left(\frac{1}{2}\right)^{\delta_{ij}} \cdot (\sum_k (M_{kj} P_k E_k SI_i + M_{ki} P_k E_k SI_j)) - (\lambda_i + \lambda_j) II_{ij} \end{aligned} \tag{21}$$

Model 5

Following Shirreff et al. (2011), Model 5 is an implicit instantaneous partnership formation model that uses an adjusted transmission rate, β', that is derived from Hollingsworth et al. (2008)'s approximate basic reproduction number:

$$\beta_i' = \frac{c\beta_i}{c + \beta_i + \lambda_i}. \tag{22}$$

Thus, we get the following model:

$$\begin{aligned} S' &= \sum_k \lambda_k I_k - \sum_k \beta_k' S I_k \\ I_i &= \sum_k M_{ki} \beta_k' S I_k - \lambda_i I_i \end{aligned} \tag{23}$$

Model 6

Model 6 is a random mixing model. It is modeled in a same way as model 6 without the adjusted transmission rate:

$$\begin{aligned} S' &= \sum_k \lambda_k I_k - \sum_k \beta_k S I_k \\ I_i &= \sum_k M_{ki} \beta_k S I_k - \lambda_i I_i \end{aligned} \tag{24}$$

Initial distribution of infected individuals

We follow Champredon et al's result to calculate the initial distribution of infected individuals. For model 1 and 2, we have disease equilibrium state of $S^* = \frac{c}{c+\rho}$ and $SS^* = \frac{1-S^*}{2}$. We let $\epsilon = 10^{-4}$, which is the total number of infected individuals in the beginning of simulation and D be the vector such that D_i represent the proportion of individuals with $\log_{10}$ SPVL of i. Y_i is taken from normal distribution with mean 3 and is normalized so that $\sum_i D_i = 1$. Then, we have the following initial distribution of each states:

$$\begin{aligned} S(0) &= (1-\epsilon)S^* \\ SS(0) &= (1-\epsilon)^2 SS^* \\ SI_i(0) &= 2\epsilon(1-\epsilon)SS^* D_i \\ I_i(0) &= \epsilon S^* D_i \\ II_{ij}(0) &= \left(\frac{1}{2}\right)^{\delta_{ij}} 2\epsilon^2 SS^* D_i D_j. \end{aligned} \tag{25}$$

Since model 3 and 4 do not have single state, $SS^* = 1$ at the disease free equilibrium and the initial distribution becomes as follows:

$$\begin{aligned} SS(0) &= (1-\epsilon)^2 SS^* \\ SI_i(0) &= 2\epsilon(1-\epsilon)SS^* D_i \\ II_{ij}(0) &= \left(\frac{1}{2}\right)^{\delta_{ij}} 2\epsilon^2 SS^* D_i D_j. \end{aligned} \tag{26}$$

Lastly, as model 5 is an implicit model, which does not consider different stages of partnership, we have the following initial distribution.

$$\begin{aligned} S(0) &= 1 - \epsilon \\ I_i(0) &= \epsilon D_i. \end{aligned} \tag{27}$$

Model 6 also shares the same distribution of initial infected individuals as model 5.

References

Alizon, S. (2009, May). The Price equation framework to study disease within-host evolution. *Journal of Evolutionary Biology 22*(5), 1123–1132.

Alizon, S. and Y. Michalakis (2015, January). Adaptive virulence evolution: the good old fitness-based approach. *Trends in Ecology & Evolution 30*(5), 248–254.

Alizon, S., V. v. Wyl, T. Stadler, R. D. Kouyos, S. Yerly, B. Hirschel, J. Bni, C. Shah, T. Klimkait, H. Furrer, A. Rauch, P. L. Vernazza, E. Bernasconi, M. Battegay, P. Brgisser, A. Telenti, H. F. Gnthard, S. Bonhoeffer, and t. S. H. C. Study (2010, September). Phylogenetic approach reveals that virus genotype largely determines HIV set-point viral load. *PLOS Pathog 6*(9), e1001123.

Blower, S. M., D. Hartel, H. Dowlatabadi, R. M. Anderson, and R. M. May (1991, February). Drugs, sex and HIV: A mathematical model for New York City. *Philosophical Transactions of the Royal Society of London B: Biological Sciences 331*(1260), 171–187.

Champredon, D., S. Bellan, and J. Dushoff (2013, 12). HIV sexual transmission is predominantly driven by single individuals rather than discordant couples: A model-based approach. *PLoS ONE 8*(12), e82906.

Day, T. and S. R. Proulx (2004, April). A general theory for the evolutionary dynamics of virulence. *The American Naturalist 163*(4), E40–E63.

De Roode, J. C., A. J. Yates, and S. Altizer (2008). Virulence-transmission trade-offs and population divergence in virulence in a naturally occurring butterfly parasite. *Proceedings of the National Academy of Sciences 105*(21), 7489–7494.

Dwyer, G., S. Levin, and L. Buttel (1990). A simulation model of the population dynamics and evolution of myxomatosis. *Ecol Monog 60*, 423–447.

Ebert, D. (1999). The evolution and expression of parasite virulence. In S. C. Stearns (Ed.), *Evolution in Health & Disease*, Chapter 14, pp. 161–172. New York: Oxford University Press, Oxford, UK.

Ebert, D. and J. J. Bull (2003). Challenging the trade-off model for the evolution of virulence: is virulence management feasible? *Trends Microbiol 11*(1), 15–20.

Elderd, B. D., V. M. Dukic, and G. Dwyer (2006, October). Uncertainty in predictions of disease spread and public health responses to bioterrorism and emerging diseases. *Proceedings of the National Academy of Sciences 103*(42), 15693 –15697.

Faria, N. R., A. Rambaut, M. A. Suchard, G. Baele, T. Bedford, M. J. Ward, A. J. Tatem, J. D. Sousa, N. Arinaminpathy, J. Ppin, D. Posada, M. Peeters, O. G. Pybus, and P. Lemey (2014, October). The early spread and epidemic ignition of HIV-1 in human populations. *Science (New York, N.Y.) 346*(6205), 56–61.

Fraser, C., T. D. Hollingsworth, R. Chapman, F. de Wolf, and W. P. Hanage (2007). Variation in HIV-1 set-point viral load: Epidemiological analysis and an evolutionary hypothesis. *PNAS 104*, 17441–17446.

Fraser, C., K. Lythgoe, G. E. Leventhal, G. Shirreff, T. D. Hollingsworth, S. Alizon, and S. Bonhoeffer (2014, March). Virulence and pathogenesis of HIV-1 infection: An evolutionary perspective. *Science 343*(6177), 1243727.

Gras, L., S. Jurriaans, M. Bakker, A. van Sighem, D. Bezemer, C. Fraser, J. Lange, J. M. Prins, B. Berkhout, F. de Wolf, et al. (2009). Viral load levels measured at set-point have risen over the last decade of the HIV epidemic in the Netherlands. *PLoS One 4*(10), e7365.

Herbeck, J., J. Mittler, G. Gottlieb, S. Goodreau, J. Murphy, A. Cori, M. Pickles, and C. Fraser (2016). Evolution of HIV virulence in response to widespread scale up of antiretroviral therapy: a modeling study. *bioRxiv*, 039560.

Herbeck, J. T., J. E. Mittler, G. S. Gottlieb, and J. I. Mullins (2014, June). An HIV epidemic model based on viral load dynamics: Value in assessing empirical trends in HIV virulence and community viral load. *PLoS Comput Biol 10*(6), e1003673.

Herbeck, J. T., V. Mller, B. S. Maust, B. Ledergerber, C. Torti, S. Di Giambenedetto, L. Gras, H. F. Gnthard, L. P. Jacobson, J. I. Mullins, and G. S. Gottlieb (2012, January). Is the virulence of HIV changing? A meta-analysis of trends in prognostic markers of HIV disease progression and transmission. *AIDS (London, England) 26*(2), 193–205.

Hollingsworth, T. D., R. M. Anderson, and C. Fraser (2008, September). HIV-1 transmission, by stage of infection. *Journal of Infectious Diseases 198*(5), 687–693.

Jensen, K. H., T. Little, A. Skorping, and D. Ebert (2006). Empirical support for optimal virulence in a castrating parasite. *PLoS Biol 4*(7), e197.

Leventhal, G. E. and S. Bonhoeffer (2016, April). Potential pitfalls in estimating viral load heritability. *bioRxiv*, 046797.

Lipsitch, M. and M. A. Nowak (1995, June). The evolution of virulence in sexually-transmitted HIV/AIDS. *J Theor Biol 174*(4), 427–440.

Lythgoe, K. A., L. Pellis, and C. Fraser (2013). Is HIV short-sighted? insights from a multistrain nested model. *Evolution 67*(10), 2769–2782.

Ma, J., J. Dushoff, B. M. Bolker, and D. J. D. Earn (2014). Estimating initial epidemic growth rates. *Bulletin of Mathematical Biology 76*(1), 245–260.

Mackinnon, M. J. and A. F. Read (1999). Genetic relationships between parasite virulence and transmission in the rodent malaria *Plasmodium chabaudi*. *Evolution*, 689–703.

Müller, V., F. Maggiolo, F. Suter, N. Ladisa, A. De Luca, A. Antinori, L. Sighinolfi, E. Quiros-Roldan, G. Carosi, and C. Torti (2009). Increasing clinical virulence in two decades of the Italian HIV epidemic. *PLoS Pathog 5*(5), e1000454.

Payne, R., M. Muenchhoff, J. Mann, H. E. Roberts, P. Matthews, E. Adland, A. Hempenstall, K.-H. Huang, M. Brockman, Z. Brumme, M. Sinclair, T. Miura, J. Frater, M. Essex, R. Shapiro, B. D. Walker, T. Ndungu, A. R. McLean, J. M. Carlson, and P. J. R. Goulder (2014, December). Impact of HLA-driven HIV adaptation on virulence in populations of high HIV seroprevalence. *Proceedings of the National Academy of Sciences 111*(50), E5393–E5400.

Shirreff, G., L. Pellis, O. Laeyendecker, and C. Fraser (2011, October). Transmission selects for HIV-1 strains of intermediate virulence: A modelling approach. *PLoS Computational Biology 7*(10), e1002185. WOS:000297262700019.

van Dorp, C. H., M. van Boven, and R. J. De Boer (2014). Immuno-epidemiological modeling of HIV-1 predicts high heritability of the set-point virus load, while selection for CTL escape dominates virulence evolution. *PLoS Computational Biology 10*(12), e1003899.

Wallinga, J. and M. Lipsitch (2007, February). How generation intervals shape the relationship between growth rates and reproductive numbers. *Proceedings of the Royal Society of London B: Biological Sciences 274*(1609), 599–604.

Wawer, M. J., R. H. Gray, N. K. Sewankambo, D. Serwadda, X. Li, O. Laeyendecker, N. Kiwanuka, G. Kigozi, M. Kiddugavu, T. Lutalo, et al. (2005). Rates of HIV-1 transmission per coital act, by stage of HIV-1 infection, in Rakai, Uganda. *Journal of Infectious Diseases 191*(9), 1403–1409.

Table 1: Parameter ranges/values. Note that c and ρ values are doubled from Champredon et al. because we keep track of individuals, while they keep track of couples. Starred (*) parameters (used in Figure 1) are from Shirreff et al..

Notation	Description	Range/Value	Source
ρ	Partnership formation rate	1/10-2/5	Champredon et al. (2013)
c	Partnership dissolution rate	1/15-1/5 (1.25*)	Champredon et al. (2013)
c_u/c_w	Relative contact rate for uncoupled transmission	1/5-5	Assumption
c_e/c_w	Relative contact rate extra-couple	0.01-1	Champredon et al. (2013)
β_P	Rate of transmission during primary infection	1.31-5.09 (2.76*)	Hollingsworth et al. (2008)
β_D	Rate of transmission during high transmission disease stage	0.413-1.28 (0.76*)	Hollingsworth et al. (2008)
D_P	Duration of primary infection	1.23/12-6/12 (0.25*)	Hollingsworth et al. (2008); Shirreff et al. (2011)
D_D	Duration of high transmission disease stage	4.81/12-14/12 (0.75*)	Hollingsworth et al. (2008)
β_{max}	Maximum rate of transmission during asymptomatic stage	0.317	Shirreff et al. (2011)
β_{50}	SPVL at which infectiousness is half maximum	13938	Shirreff et al. (2011)
β_k	Hill coefficient: steepness of increase in infectiousness as a function of SPVL	1.02	Shirreff et al. (2011)
D_{max}	Duration of primary infection	25.4	Shirreff et al. (2011)
D_{50}	SPVL at which duration of asymptomatic infection is half maximum	3058	Shirreff et al. (2011)
D_k	Hill coefficient: steepness of decrease in duration as a function of SPVL	0.41	Shirreff et al. (2011)
σ_M	Mutation standard deviation of $\log_{10}$ SPVL	0.12	Shirreff et al. (2011)
α_{min}	Minimum $\log_{10}$ SPVL	2	Shirreff et al. (2011)
α_{max}	Maximum $\log_{10}$ SPVL	7	Shirreff et al. (2011)
n	Number of strains	21 (51*)	Assumption